Earthquakes and Structures, *Vol. 16, No. 3 (2019) 359-368*
DOI: https://doi.org/10.12989/eas.2019.16.3.359

Dynamic behaviour of thick plates resting on Winkler foundation with fourth order element

Yaprak I. Özdemir*

Department of Civil Engineering, Karadeniz Technical University, 61080 Trabzon, Turkey

(Received November 28, 2018, Revised February 8, 2019, Accepted February 19, 2019)

Abstract. This paper focuses on the study of dynamic analysis of thick plates resting on Winkler foundation. The governing equation is derived from Mindlin's theory. This study is a parametric analysis of the reflections of the thickness / span ratio, the aspect ratio and the boundary conditions on the earthquake excitations are studied. In the analysis, finite element method is used for spatial integration and the Newmark-β method is used for the time integration. While using finite element method, a new element is used. This element is 17-noded and it's formulation is derived from using higher order displacement shape functions. C++ program is used for the analyses. Graphs are presented to help engineers in the design of thick plates subjected to earthquake excitations. It is concluded that the 17-noded finite element is used in the earthquake analysis of thick plates. It is shown that the changes in the aspect ratio are more effective than the changes in the aspect ratio. The center displacements of the reinforced concrete thick clamped plates for b/a=1, and t/a=0.2, and for b/a=2, and t/a=0.2, reached their absolute maximum values of 0.00244 mm at 3.48 s, and of 0.00444 mm at 3.48 s, respectively.

Keywords: free vibration analysis; forced vibration analysis; Newmark method; Mindlin's theory; fourth order finite element; Winkler foundation

1. Introduction

One of the important design elements are rectangular plates in different branches of modern engineering fields including mechanical, aerospace, optical and structural engineering. It is popular for the design of many engineering problems, such as the vibration behavior of reinforced concrete plates on elastic foundations, foundations of buildings, asphalting of roads and soles of machines. The mechanical behavior of foundation was widely discussed by Winkler (1868), Pasternak (1954), Hetenyi (1950), Vlasov and Leont'ev (1989).

Winkler type elastic foundation is the simplest model to describe the mechanical behavior of elastic supports. In this model a set of uncorrelated elastic springs attached to each node of the plate (Winkler 1868).and interaction between lateral springs are ignored. Pasternak (1954) developed two-parameter elastic foundation models to consider this interaction. Vlasov and Leont'ev (1989) derived a solution which is calculated with soil material and thickness of the soil with a γ parameter.

Different investigations have been done by many researchers (Senjanovic *et al*. 2017, Zamani *et al*. 2017, Karasin 2016, Zhang *et al*. 2016, Tahouneh 2014, Grice and Pinnington 2002, Lok and Cheng 2001, Si *et al*. 2005, Wu 2012, Kutlu *et al*. 2012, Sheikholeslami and Saidi 2013) about the dynamic behavior of thick elastic plates. The free vibration of thin plates resting on Pasternak foundation wit finite element method was studied by Omurtag *et al*. (1997). Wu and Lee (2011) investigated the dynamic response of a homogeneous, isotropic and elastic circular plate on an elastic foundation subjected to axisymmetric time dependent loads both analytically and numerically. Wirowski *et al*. (2015) derived an averaged mathematical model to study the dynamic behavior of the composite annular plates resting on elastic heterogeneous foundation with two foundation modules. Zenkour and Radwan (2016) used four-variable refined plate theory for free vibration of laminated composite and soft core sandwich plates resting on Winkler–Pasternak foundations.

Shear locking problem occurs at thick plates (Zienkiewich *et al*. 1971) while the thickness becomes smaller. This problem can be avoided by increasing the mesh size, i.e., using finer mesh, but convergence may not be achieved if the thickness/span ratio is "too small", for the first and second order displacement shape functions. It can increase the accuracy of finite element solutions after refining the finite element mesh or using high order shape functions. These problems can be prevented with using true shape function while built up the mathematical model. The author formed a new 17 noded, 4 order shape function finite element at the past studies and this element is free from shear locking (Ö zdemir *et al*. 2007) and also author used this element at another study for thick plates resting on Winkler foundation (Ö zdemir 2012) This element is a new element for literature and there isn't any research about the free vibration nor forced vibration analysis of thick plates resting on Winkler foundation with higher order finite elements.

The aim of this study is to investigate dynamic behavior of Mindlin plates based on Winkler foundation and, to

*Corresponding author, Associate Professor
E-mail: yaprakozdemir@hotmail.com

ISSN: 2092-7614 (Print), 2092-7622 (Online)

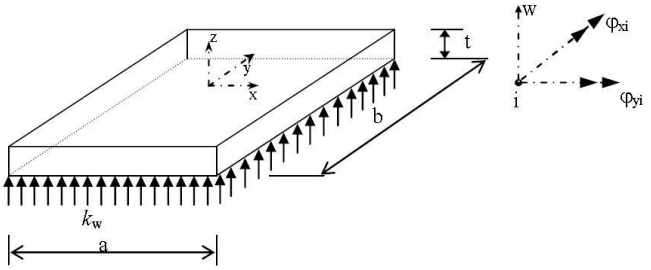

Fig. 1 The sample plate used in this study

determine the effects of the thickness/span ratio, the aspect ratio and the boundary conditions on the linear responses of the reinforced concrete thick plates subjected to earthquake excitations. At the analysis a computer program is derived with C++ and in the program, the finite element method is used for spatial integration and the Newmark-β method is used for the time integration. Higher order displacement shape functions are used for finite element modeling of plate. In the analysis, 17-noded finite element is used to construct the stiffness and mass matrices since shear locking problem does not occur if this element is used in the finite element modelling of the thick plates (Ö zdemir *et al*. 2007). No matter what the mesh size is unless it is less than 4×4. This is a new element, details of its formulation are presented in (Ö zdemir *et al*. 2007) and this is the first time this element is used in the forced vibration of reinforced concrete thick plates resting Winkler foundation in the literature. If this element is used in an analysis, it is not necessary to use finer mesh.

2. Mathematical model

The governing equation for a flexural plate (Fig. 1) subjected to an earthquake excitation without damping can be given as (Ayvaz *et al*. 1995, Tedesco *et al*. 1999)

$$[M]\{\ddot{w}\}+[K]\{w\}=[F]=-[M]\{\ddot{u}_g\} \tag{1}$$

where [*K*] and [*M*] are the stiffness matrix and the mass matrix of the plate, respectively, w and ẅ are the lateral displacement and the second derivative of the lateral displacement of the plate with respect to time, respectively, $\ddot{u}_g$ is the earthquake acceleration.

Forced vibration analysis of a plate can be made by constructed with the stiffness, [*K*], mass matrices, [*M*], and equivalent nodal loads vector, [*F*], of the plate. The evaluation of these matrices is given in the following sections.

The total strain energy of plate-soil-structure system (see Fig. 1) can be written as

$$\Pi=\Pi_p+\Pi_s+V \tag{2}$$

where Π_p is the strain energy in the plate

$$\prod_p=\frac{1}{2}\int_A\left(-\frac{\partial\varphi_x}{\partial x}\quad\frac{\partial\varphi_y}{\partial y}\quad-\frac{\partial\varphi_x}{\partial y}+\frac{\partial\varphi_y}{\partial x}\right)^T E_\kappa\left(-\frac{\partial\varphi_x}{\partial x}\quad\frac{\partial\varphi_y}{\partial y}\quad-\frac{\partial\varphi_x}{\partial y}+\frac{\partial\varphi_y}{\partial x}\right)dA+$$
$$\frac{k}{2}\int_A\left(-\varphi_x+\frac{\partial w}{\partial x}\quad\varphi_y+\frac{\partial w}{\partial y}\right)^T E_\gamma\left(-\varphi_x+\frac{\partial w}{\partial x}\quad\varphi_y+\frac{\partial w}{\partial y}\right)dA- \tag{3}$$

where Π_s is the strain energy stored in the soil

$$\prod_s=\frac{1}{2}\int_0^H\int_{-\infty}^{\infty}\int_{-\infty}^{\infty}\sigma_{ij}\varepsilon_{ij} \tag{4}$$

and *V* is the potential energy of the earthquake loading

$$V=-\int_A\bar{q}w\,dA \tag{5}$$

In this equation E_κ and E_γ are the elasticity matrix and these matrices are given below at Eq. (14), $\bar{q}$ shows earthquake loading.

2.1 Regulation of the stiffness matrix

The total strain energy of the plate-soil system according to Eq. (2) is

$$U_e=\frac{1}{2}\int_A\left(-\frac{\partial\varphi_x}{\partial x}\quad\frac{\partial\varphi_y}{\partial y}\quad-\frac{\partial\varphi_x}{\partial y}+\frac{\partial\varphi_y}{\partial x}\right)^T E_\kappa\left(-\frac{\partial\varphi_x}{\partial x}\quad\frac{\partial\varphi_y}{\partial y}\quad-\frac{\partial\varphi_x}{\partial y}+\frac{\partial\varphi_y}{\partial x}\right)dA+$$
$$+\frac{k}{2}\int_A\left(-\varphi_x+\frac{\partial w}{\partial x}\quad\varphi_y+\frac{\partial w}{\partial y}\right)^T E_\gamma\left(-\varphi_x+\frac{\partial w}{\partial x}\quad\varphi_y+\frac{\partial w}{\partial y}\right)dA$$
$$+\frac{1}{2}\int_A\left(w_{x,y}\right)^T\mathrm{K}\left(w_{x,y}\right)dA \tag{6}$$

At this equation the first and second part gives the conventional element stiffness matrix of the plate, [k_p^e], differentiation of the third integral with respect to the nodal parameters yields a matrix, [k_w^e], which accounts for the axial strain effect in the soil. Thus the total energy of the plate-soil system can be written as

$$U_e=\frac{1}{2}\{w_e\}^T\left(\left[k_p^e\right]+\left[k_w^e\right]\right)\{w_e\}dA \tag{7}$$

where

$$\{w_e\}=\left[w_1\quad\varphi_{y1}\quad\varphi_{x1}\quad\ldots\quad w_n\quad\varphi_{yn}\quad\varphi_{xn}\right]^T \tag{8}$$

Assuming that in the plate of Fig. 1 *u* and *v* are proportional to *z* and that *w* is the independent of *z* (Mindlin 1951), one can write the plate displacement at an arbitrary *x*, *y*, *z* in terms of the two slopes and a displacement as follows

$$u_i=\{w, v, u\}=\{w_{0(x,y,t)}, z\varphi_{y(x,y,t)}, -z\varphi_{x(x,y,t)}\} \tag{9}$$

where w_0 is average displacement of the plate, and φ_x and φ_y are the bending slopes in the *x* and *y* directions, respectively.

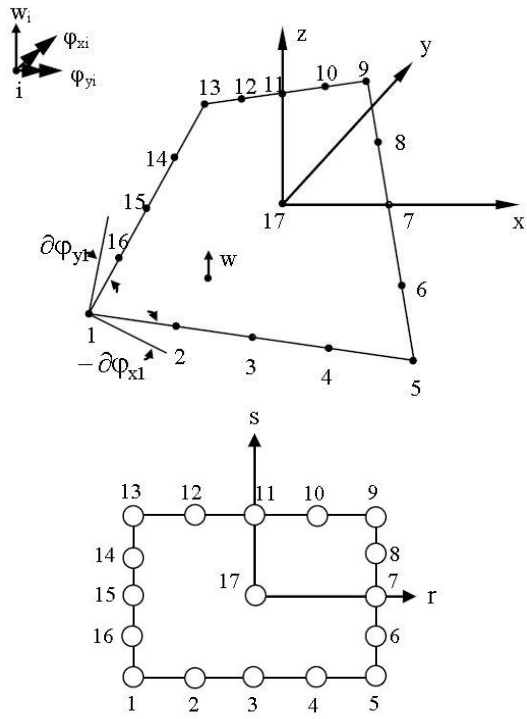

Fig. 2 17-noded quadrilateral finite element used in this study (Özdemir *et al*. 2007)

The nodal displacements for 17-noded quadrilateral serendipity element (MT17) (Fig. 2) can be written as follows

$$w=\sum_{1}^{17} h_i w_i \ , \ v=z\varphi_y=z\sum_{1}^{17} h_i \varphi_{yi} \ , \ u=-z\varphi_x=-z\sum_{1}^{17} h_i \varphi_{xi}$$
$$i=1,...,17 \text{ for } 17\text{ - noded element}, \quad (10)$$

if displacement function derived for 17-noded element

$$w = c_1 + c_2 r + c_3 s + c_4 r^2 + c_5 rs + c_6 s^2 + c_7 r^2 s + c_8 rs^2 + c_9 r^3 + c_{10} r^3 s + c_{11} rs^3 + c_{12} s^3 + c_{13} r^2 s^2 + c_{14} r^4 + c_{15} r^4 s + c_{16} rs^4 + c_{17} s^4. \quad (11)$$

With this assumption, the displacement shape function can be formed

$$h = [h_1,..., h_{17}]. \quad (12)$$

Then, the strain-displacement matrix [*B*] for this element can be written as follows (Cook *et al.* 1989)

$$[B]=\begin{bmatrix} 0 & 0 & -\frac{\partial h_i}{\partial x} & \cdots \\ 0 & \frac{\partial h_i}{\partial y} & 0 & \cdots \\ 0 & \frac{\partial h_i}{\partial x} & -\frac{\partial h_i}{\partial y} & \cdots \\ \frac{\partial h_i}{\partial x} & 0 & -h_i & \cdots \\ \frac{\partial h_i}{\partial y} & h_i & 0 & \cdots \end{bmatrix}_{5x51}$$
$$i=1,...,17 \text{ for } 17\text{ - noded element} \quad (13)$$

The details of the matrix B for 17-noded quadrilateral finite element is presented in Özdemir *et al*. The stiffness matrix for MT17 element can be obtained by the following equation (Weaver and Johnston 1984).

$$k_p = \int_V B^T EB dV = \int_V \begin{bmatrix} z\overline{B}_k^T & B_\gamma^T \end{bmatrix} \begin{bmatrix} E_k & 0 \\ 0 & E_\gamma \end{bmatrix} \begin{bmatrix} z\overline{B}_k^T \\ B_\gamma^T \end{bmatrix} dV$$
$$k_p = \int_V \left(z^2 \overline{B}_k^T E_k \overline{B}_k \right) + \left(\overline{B}_\gamma^T E_\gamma \overline{B}_\gamma \right) dV. \quad (14)$$

Integration of Eq. (14) through the thickness yields

$$k_p = \int_A \left(\overline{B}_k^T \overline{E}_k \overline{B}_k + \overline{B}_\gamma^T \overline{E}_\gamma \overline{B}_\gamma \right) dA \quad (15)$$

where the first term concerns with the bending and the second term concerns with the shear effects of the thick plate. Thus

$$k_p = \int_A \overline{B}^T \overline{E} \overline{B} dA = \int_{-1}^{1}\int_{-1}^{1} \overline{B}^T \overline{E} \overline{B} |J| drds \quad (16)$$

which must be evaluated numerically (Bathe 1996).

2.2 Elastic foundation formulation

Winkler type elastic foundation is the simplest model to describe the mechanical behavior of elastic supports. In this model a set of uncorrelated elastic springs attached to each node of the plate and interaction between lateral springs are ignored. Winkler foundation stiffness matrices can be derived by

$$k_w = k \int_{-1}^{1}\int_{-1}^{1} [h]^T [h] |J| drds \quad (17)$$

where *k* is the elastic foundation modulus.

After calculating all element stiffness matrices, global stiffness matrix can be assembled as;

$$[K] = \sum_{i=1}^{p_e} \left([k_p] + [k_w] \right) \quad (18)$$

where p_e is the node number.

2.3 Regulation of the mass matrix

The consistent mass matrix formulation of the plate may be written as

$$M = \int_\Omega H_i^T \mu H_i d\Omega \quad (19)$$

In this equation, μ is the mass density matrix of the form (Tedesco *et al.* 1999)

$$\mu = \begin{bmatrix} m_1 & 0 & 0 \\ 0 & m_2 & 0 \\ 0 & 0 & m_3 \end{bmatrix}, \quad (20)$$

where $m_1=\rho_p t$, $m_2=m_3=\frac{1}{12}\left(\rho_p t^3\right)$, and ρ_p is the mass densities of the plate. and H_i can be written as follows

$$H_i = \left[dh_i / dx \quad dh_i / dy \quad h_i \right] \qquad i = 1 \ldots 17 \ldots \qquad (21)$$

It should be noted that the rotation inertia terms are not taken into account. By assembling the element mass matrices obtained, the system mass matrix is obtained.

2.4 Regulation of equivalent nodal loads vector

Equivalent nodal loads, [*F*], can be obtained by the following equation.

$$[F] = \int H_i^T \bar{q} d\Omega \qquad (22)$$

In this equation, H_i can be obtained by Eq. (21), and $\bar{q}$ denotes

$$\bar{q} = -[M]\{\ddot{u}_g\} \qquad (23)$$

In this study for the eigenvalue solution of Eq. (1) the program MATLAB is used and also the Newmark-β method is used by using the average acceleration method for the time integration of Eq. (2).

2.5 Evaluation of frequency of plate

The formulation of lateral displacement, *w*, can be given as motion is sinusoidal

$$w = W \sin \omega t \qquad (24)$$

Here ω is the circular frequency. Substitution of Eq. (24) and its second derivation into Eq. (1) gives expression as

$$[K - \omega^2 M]\{W\} = 0 \qquad (25)$$

Eq. (25) is obtained to calculate the circular frequency, ω, of the plate. Then natural frequency can be calculated with the formulation below

$$f = \omega / 2\pi \qquad (26)$$

The flowchart of the developed program is given below;

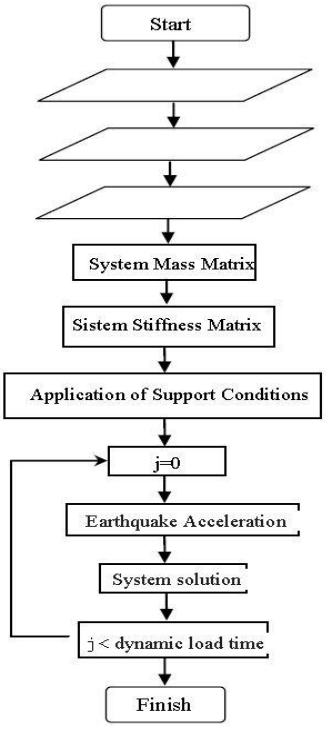

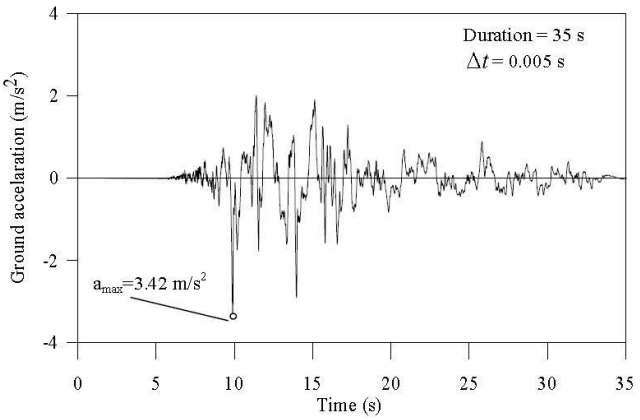

Fig. 3 YPT330 component of the August 17, 1999 Kocaeli earthquake in Turkey

3. Numerical examples

3.1 Data for numerical examples

In the light of the results given in references (Ö zdemir *et al.* 2007, Ö zdemir 2007), the aspect ratios, b/a, of the plate are taken to be 1.0, 2.0, and 3.0. The thickness/span ratios, t/a, are taken as 0.05, 0.1, 0.2, and 0.3 for each aspect ratio. The shorter span length of the plate is kept constant to be 3 m. The plates are clamped and simply supported along four edges. The mass density, Poisson's ratio, and the modulus of elasticity of the reinforced concrete plate are taken to be 2.5 kN s^2/m^2, 0.2, and 2.7×10^7 kN/m^2. Shear factor *k* is taken to be 5/6. The subgrade reaction modulus of the Winkler-type foundation is taken to be 500, 5000, 50000 kN/m^3.

In the time history analysis to obtain the response of each plate the first 20 s of YPT330 component of the August 17,1999 Kocaeli earthquake in Turkey is used. The earthquake –induced ground motion is applied at the vertical direction of the plate. Duration of this earthquake is 35 s, but the peak value of the record occurred in the first 20 s of the earthquake (Fig. 3).

For the sake of accuracy in the results, rather than starting with a set of a finite element mesh size and time increment, the mesh size and time increment required to obtain the desired accuracy were determined before presenting any results This analysis was performed separately for the mesh size and time increment. It was concluded that the results have acceptable error when equally spaced 4×4 mesh sizes are used for a 3 m×3 m plate, if the 0.005 s time increment is used. In the analysis length of each finite elements in the x and y directions are kept constant for different aspect ratios as in the form of square reinforced concrete plate.

3.2 Results

One of the purposes of this paper was to determine the time histories of the displacements and the bending moments at different points of the thick plates subjected to earthquake excitations, but presentation of all of the time histories would take up excessive space. Hence, only the

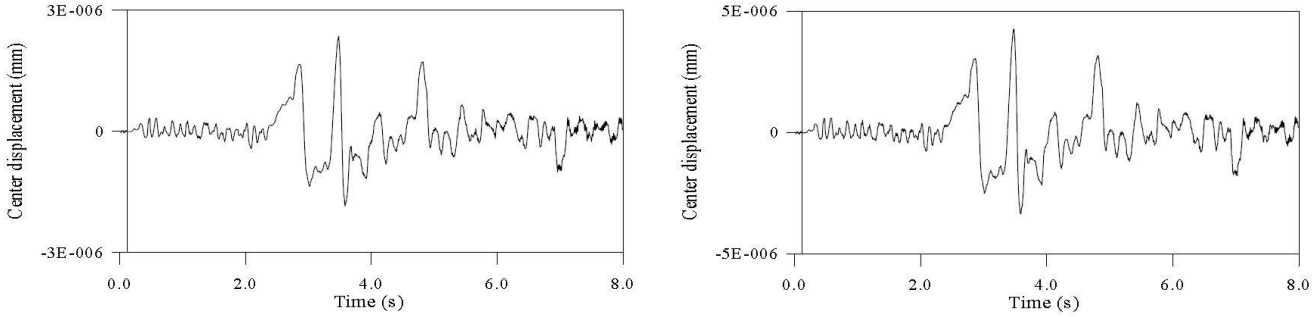

(a) (b)

Fig. 4 The time history of the center displacement of the reinforced concrete thick clamped plate resting on Winkler foundation for (a) *b/a*=1.0 and *t/a*=0.2, and (b) *b/a*=2.0 and *t/a*=0.2

Table 1 Effects of aspect ratio and thickness/span ratio on the absolute maximum displacement and absolute maximum bending moment of the reinforced concrete thick simply supported plates resting on elastic foundation

k	*t/a*	*b/a*=1			*b/a*=2			*b/a*=3		
		w (mm)	M_x (kNmm)	M_y (kNmm)	*w* (mm)	M_x (kNmm)	M_y (kNmm)	*w* (mm)	M_x (kNmm)	M_y (kNmm)
5000	0.05	0.0632	597	597	0.1139	964	327	0.1392	1170	309
	0.10	0.0169	1226	1226	0.0407	2735	1002	0.0452	2991	722
	0.20	0.00503	2508	2508	0.011	5484	1996	0.012	5918	1395
	0.30	0.00268	3984	3984	0.0056	8696	3168	0.0061	9195	2202

Table 2 Effects of aspect ratio and thickness/span ratio on the absolute maximum displacement and absolute maximum bending moment of the reinforced concrete thick clamped plates resting on elastic foundation

k	*t/a*	*b/a*=1			*b/a*=2			*b/a*=3		
		w (mm)	M_x (kNmm)	M_y (kNmm)	*w* (mm)	M_x (kNmm)	M_y (kNmm)	*w* (mm)	M_x (kNmm)	M_y (kNmm)
5000	0.05	0.0252	359	359	0.0388	534	160	0.0405	559	129
	0.10	0.0071	721	721	0.0104	1054	326	0.0107	1080	237
	0.20	0.0024	1442	1442	0.0033	1999	653	0.0035	1989	416
	0.30	0.0016	2198	2198	0.0021	3019	1091	0.0022	3199	713

absolute maximum displacements and bending moments for different thickness/span ratio and aspect ratio are presented after two time One of the purposes of this study was to study earthquake behavior of the thick plates with elastic foundation and to determine the time histories of the displacements and the bending moments at different points of these thick plates, but presentation of all of the time histories would take up excessive space. Because of the fact that the maximum values of displacements and bending moments are the most important ones for design these values are presented for different thickness/span ratio and aspect ratio after two time histories are given. These results are presented in graphical rather than in tabular form.

The time histories of the center displacements of the thick clamped plates resting on elastic foundation with the subgrade reaction modulus of the Winkler-type foundation 5000 kN/m^3 for *b/a*=1.0, and 2.0 when *t/a*=0.2 are given in Figs. 4(a), and 4(b), respectively.

As seen from Figs. 4(a), and 4(b), the center displacements of the reinforced concrete thick clamped plates for *b/a*=1, and *t/a*=0.2, and for *b/a*=2, and *t/a*=0.2, reached their absolute maximum values of 0.00244 mm at 3.48 s, and of 0.00444 mm at 3.48 s, respectively. These absolute maximum values are different even with the same occurring time as the dynamic characteristics of the

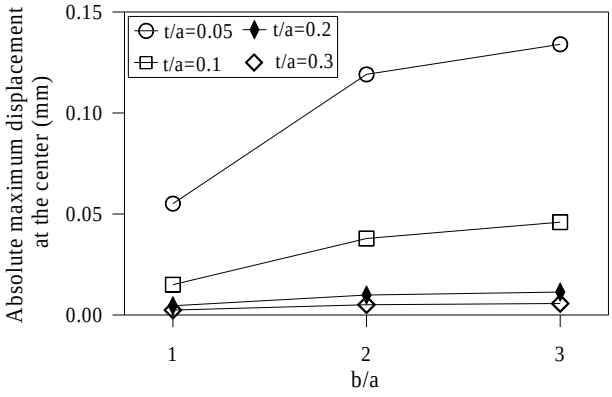

Fig. 5 Absolute maximum displacement of the reinforced concrete thick simply supported plates resting on Winkler foundation for different aspect ratios and thickness/span ratios

reinforced concrete thick plates affect the response. It is also understandable that the system becomes more flexible as the aspect ratio increases.

The absolute maximum displacements of the thick plates for different aspect ratios, and thickness/span ratios are given in Table 1, Fig. 5 for the reinforced concrete thick plates simply supported along all four edges, in Table 2,

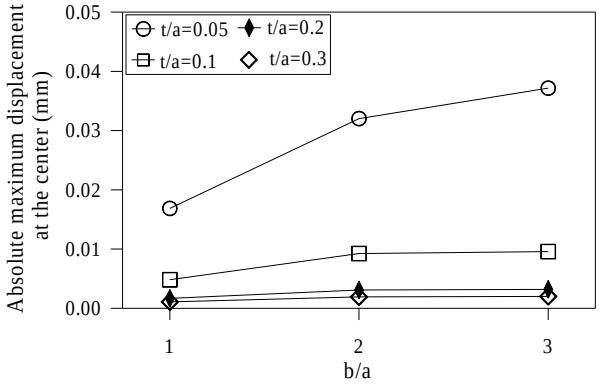

Fig. 6 Absolute maximum displacement of the reinforced concrete thick clamped plates resting on Winkler foundation for different aspect ratios and thickness/span ratios

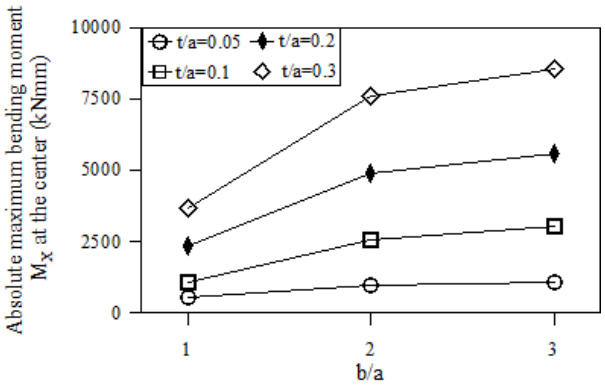

Fig. 7 Absolute maximum bending moment M_x at the center of the reinforced concrete thick simply supported plates resting on Winkler foundation for different aspect ratios and thickness/span ratios

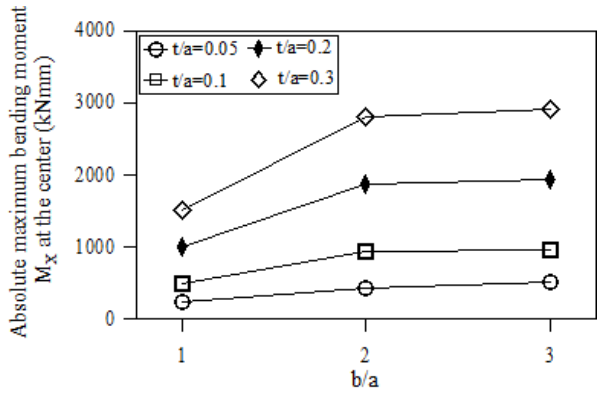

Fig. 8 Absolute maximum bending moment M_x at the center of the reinforced concrete thick clamped plates resting on Winkler foundation for different aspect ratios and thickness/span ratios

Fig. 6 for the thick plates clamped along all four edges, and in Table 3 for the thick plates free along all four edges.

As seen from Tables 1, 2 and Figs. 5, and 6, the absolute maximum displacements of the reinforced concrete thick plates increase with increasing aspect ratio for a constant *t/a* ratio. The same displacements decrease with increasing *t/a* ratio for a constant *b/a* ratio. As also seen from these figures, the decrease in the absolute maximum displacement for a constant *b/a* ratio increases with increasing *b/a* ratio. The curves for a constant value of the aspect ratio, *b/a* are fairly getting closer to each other as the value of *t/a* increases. This shows that the curves of the absolute maximum displacements will almost coincide with each other when the value of the thickness/span ratio, *t/a*, increases more. In other words, the increase in the thickness/span ratio will not affect the absolute maximum displacements after a determined value of *t/a*.

As seen from Tables 1, 2 and Figs. 5, and 6, the absolute maximum displacements of the reinforced concrete thick plates increase with increasing aspect ratio for a constant *t/a* ratio. The same displacements decrease with increasing *t/a* ratio for a constant *b/a* ratio. As also seen from these figures, the decrease in the absolute maximum displacement for a constant *b/a* ratio increases with increasing *b/a* ratio. The curves for a constant value of the aspect ratio, *b/a* are fairly getting closer to each other as the value of *t/a* increases. This shows that the curves of the absolute maximum displacements will almost coincide with each other when the value of the thickness/span ratio, *t/a*, increases more. In other words, the increase in the thickness/span ratio will not affect the absolute maximum displacements after a determined value of *t/a*.

As also seen from Tables 1, 2 and Figs. 5, and 6, the absolute maximum displacements of the reinforced concrete thick simply supported plates are larger than those of the thick clamped plates for the same aspect and thickness/span ratios. In general, the effects of the changes in the thickness/span ratios on the absolute maximum displacement are larger than the changes in the aspect ratios.

The absolute maximum bending moments M_x at the center of the reinforced concrete thick plates for different aspect ratios and thickness/span ratios are given in Table 1 and Fig. 7 for the thick simply supported plates in Table 2 and Fig. 8 for the thick clamped plates, and in Table 3 for the thick free plates, respectively.

As seen from Table 1 and Fig. 7, the absolute maximum bending moment, M_x, at the center of the reinforced concrete thick and thin simply supported plates increases with increasing aspect ratio and thickness/span ratio. The increases in the absolute maximum bending moment, M_x, increase with increasing aspect and thickness/span ratios. This is understandable that increasing the aspect ratio makes the plate stiffer in the short span, the *x* axis, direction. As also seen from this figure, in general, the effects of the changes in the aspect ratios on the absolute maximum bending moment, M_x, are larger than the changes in the thickness/span ratios.

As seen from Table 2 and Fig. 8, the absolute maximum bending moment, M_x, at the center of the reinforced concrete thick clamped plates, as in the case of the absolute maximum bending moment, M_x, at the center of the reinforced concrete thick simply supported plates, increases with increasing aspect ratio and thickness/span ratio. The increases in the absolute maximum bending moment, M_x, increase with increasing aspect and thickness/span ratios. This is also understandable that increasing the aspect ratio

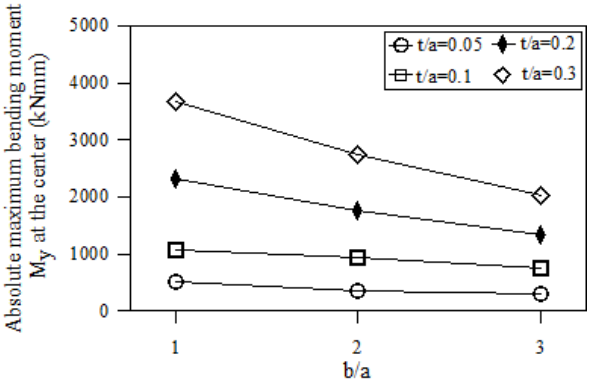

Fig. 9 Absolute maximum bending moment M_y at the center of the reinforced concrete thick simply supported plates resting on Winkler foundation for different aspect ratios and thickness/span ratios

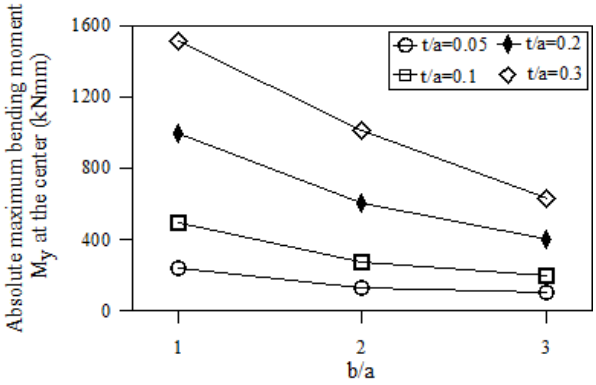

Fig. 10 Absolute maximum bending moment M_y at the center of the reinforced concrete thick clamped plates resting on Winkler foundation for different aspect ratios and thickness/span ratios

makes the plate stiffer in the short span, the x axis, direction. As also seen from this figure, in general, the effects of the changes in the aspect ratios on the absolute maximum bending moment, M_x, are larger than the changes in the thickness/span ratios.

The absolute maximum bending moments M_y at the center of the reinforced concrete thick plates for different aspect ratios and thickness/span ratios are given in Table1 and Fig. 9 for the thick and thin simply supported plates and in Table 2 and Fig. 10 for the thick clamped plates, respectively.

As seen from Table 1 and Fig. 9, the absolute maximum bending moment, M_y, at the center of the reinforced concrete thick simply supported plates decreases with increasing aspect ratio and increases with increasing thickness/span ratio. The decrease in the absolute maximum bending moment, M_y, increase with increasing aspect ratio. The increase in the absolute maximum bending moment, M_y, increases with increasing thickness/span ratios. This is understandable that increasing the aspect ratio makes the reinforced concrete thick plates more flexible in the long span, the y axis, direction. As also seen from this figure, in general, the effects of the changes in the thickness/span ratios on the absolute maximum bending moment, M_y, are larger than the changes in the aspect ratios.

As seen from Table 2 and Fig. 10, the absolute maximum bending moment, M_y, at the center of the reinforced concrete thick clamped plates, as in the case of the absolute maximum bending moment, M_y, at the center of the reinforced concrete thick simply supported plates, decreases with increasing aspect ratio and increases with increasing thickness/span ratio. The decrease in the absolute maximum bending moment, M_y, increase with increasing aspect ratio. The increase in the absolute maximum bending moment, M_y, increases with increasing thickness/span ratios. This is also understandable that increasing the aspect ratio makes the thick plates more flexible in the long span, the y axis, direction. As also seen from this figure, in general, the effects of the changes in the thickness/span ratios on the absolute maximum bending moment, M_y, are larger than the changes in the aspect ratios.

In this study, the absolute maximum bending moments M_x at the center of the edge in the y direction and the maximum bending moment M_y at the center of the edge in the x direction are not presented for the reinforced concrete thick plates clamped along all four edges. It should be noted

Table 3 Effects of aspect ratio and thickness/span ratio on the absolute maximum displacement and absolute maximum bending moment of the reinforced concrete thick free plates resting on elastic foundation

k	t/a	b/a=1			b/a=2			b/a=3		
		w (mm)	M_x (kNmm)	M_y (kNmm)	w (mm)	M_x (kNmm)	M_y (kNmm)	w (mm)	M_x (kNmm)	M_y (kNmm)
500	0.05	4.5	0.0003	0.0003	4.5	0.0005	0.0002	5.5999	0.0005	0.00009
	0.10	13.8	0.00309	0.00309	13.8	0.00584	0.00255	13.7469	0.00625	0.00443
	0.20	41.9	0.00914	0.00914	41.9404	0.03353	0.02124	41.9404	0.03148	0.02393
	0.30	66.9	0.03466	0.03466	66.9	0.04848	0.02883	66.9	0.08295	0.02873
5000	0.05	0.454	0.00034	0.00034	0.454	0.00051	0.00011	0.454	0.00054	0.00016
	0.10	1.023	0.00345	0.00345	1.023	0.00583	0.00239	1.023	0.00628	0.00475
	0.20	2.754	0.00712	0.00712	2.754	0.02707	0.01874	2.754	0.03147	0.02399
	0.30	4.127	0.03760	0.03760	4.127	0.08114	0.06445	4.127	0.08972	0.08316
50000	0.05	0.02633	0.00030	0.00030	0.02633	0.00049	0.00274	0.02633	0.00048	0.00023
	0.10	0.06189.	0.00358	0.00358	0.06189	0.00578	0.00181	0.06189	0.00627	0.00441
	0.20	0.1355	0.00923	0.00923	0.1355	0.03299	0.01439	0.1355	0.03142	0.00751
	0.30	0.2119	0.03850	0.03850	0.2119	0.08231	0.05907	0.2119	0.08479	0.07122

Table 4 Effects of aspect ratio and thickness/span ratio on the first six frequency parameters of the reinforced concrete thick free plates resting on elastic foundation

k	b/a	t/a	$\lambda=\omega^2$					
			λ_1	λ_2	λ_3	λ_4	λ_5	λ_6
5000	1.0	0.05	4049	4051	4051	8654	13834	16962
		0.10	1783	1829	1829	19105	39152	50909
		0.20	988	988	1101	59431	1274060	165228
		0.30	770	770	798	109738	230497	295940
	2.0	0.05	4045	4049	4049	4747	5184	9370
		0.10	1762	1794	1810	4571	6154	21988
		0.20	1004	1071	1118	115854	16355	69348
		0.30	764	790	791	22769	30748	127204
	3.0	0.05	4043	4047	4048	4185	4543	5100
		0.10	1754	1778	1803	2337	3706	5943
		0.20	1009	1095	1124	3231	7782	16695
		0.30	762	788	791	5467	14142	32756
50000	1.0	0.05	134259	134259	134534	185235	242522	277537
		0.10	67151	67151	67455	258471	480894	611538
		0.20	31271	31271	32953	680376	1434579	1854906
		0.30	20020	20020	21489	1230411	2570619	3298191
	2.0	0.05	134279	134465	134557	142102	146823	193349
		0.10	67095	67379	67384	97876	115120	290808
		0.20	31384	32518	33072	148898	201930	790479
		0.30	19947	21099	21417	264578	353058	1424548
	3.0	0.05	134285	134513	134564	135974	139743	146097
		0.10	67076	67360	67390	73390	88071	113293
		0.20	31422	32810	33111	56345	106679	205627
		0.30	19923	21282	21393	72866	168580	375635

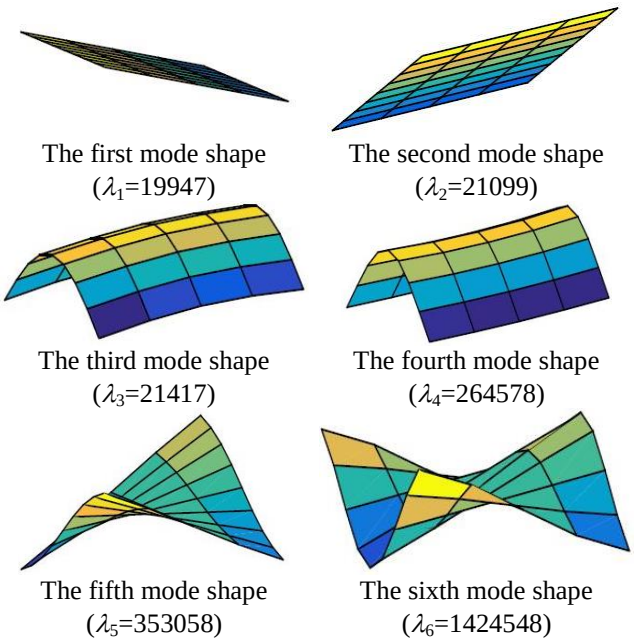

Fig. 11 The first six mode shapes of the reinforced concrete thick free plates for b/a=2.0 and t/a=0.3 with subgrade reaction modulus k=50000

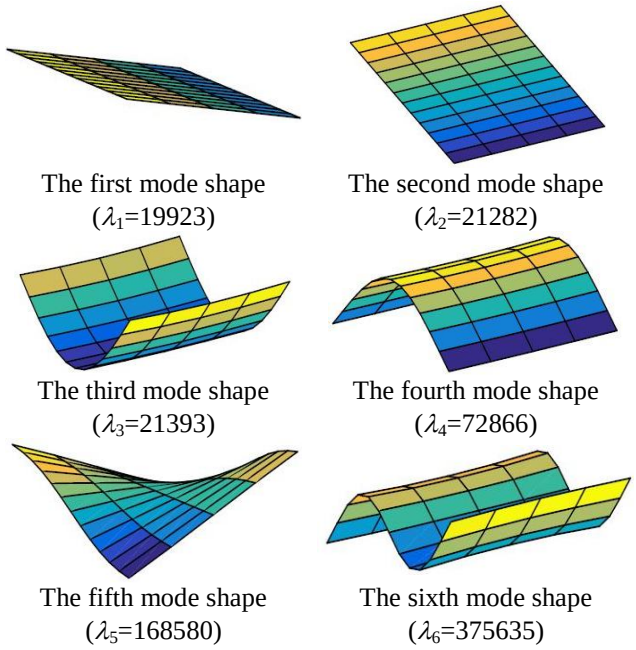

Fig. 12 The first six mode shapes of the reinforced concrete thick free plates for b/a=3.0 and t/a=0.3 with subgrade reaction modulus k=50000

that the variations of these moments are similar to the absolute maximum bending moments M_x at the center of the thick clamped plates.

The first six frequency parameters of reinforced concrete thick plates resting on Winkler foundation considered for different aspect ratio, b/a, thickness/smaller span ratio, t/a, are presented in Table 4 for the different subgrade reaction modulus with free edges. In order to see

the effects of the changes in these parameters better on the first six frequency parameters, they are also presented in Fig. 11 for the reinforced concrete thick free plates with different subgrade reaction modulus.

As seen from Table 4, the values of the first three frequency parameters for a constant value of t/a increase as the aspect ratio, *b/a*, increases up to the 3rd frequency parameters, but after the 3rd frequency parameter, the values of the frequency parameters for a constant value of *t/a* decrease as the aspect ratio, *b/a*, increases.

As also seen from Table 4, the values of the first three frequency parameters for a constant value of b/a decrease as the thickness/span ratio, *b/a*, increases up to the 3rd frequency parameters, but after the 3rd frequency parameters, the values of the frequency parameters for a constant value of *b/a* increase as the thickness/span ratio, *t/a*, increases.

The increase in the frequency parameters with increasing value of *b/a* for a constant *t/a* ratio gets less for larger values of *b/a* up to the 3rd frequency parameters. After the 3rd frequency parameters, the decrease in the frequency parameters with increasing value of *b/a* for a constant *t/a* ratio gets also less for larger values of *b/a*.

The changes in the frequency parameters with increasing value of *b/a* for a constant t/a ratio is larger for the smaller values of the *b/a* ratios. Also, the changes in the frequency parameters with increasing value of *b/a* for a constant *t/a* ratio is less than that in the frequency parameters with increasing increasing *t/a* ratios for a constant value of *b/a*.

These observations indicate that the effects of the change in the *t/a* ratio on the frequency parameter of the reinforced concrete plate are generally larger than those of the change in the *b/a* ratios considered in this study.

In this study, the mode shapes of the reinforced concrete thick plates are also obtained for all parameters considered. Since presentation of all of these mode shapes would take up excessive space, only the mode shapes corresponding to the six lowest frequency parameters of the reinforced concrete thick plate free along all four edges for *b/a* 2, and 3 and *t/a*=0.3, are presented. These mode shapes are given in Figs. 11, and 12, respectively. In order to make the visibility better, the mode shapes are plotted with exaggerated amplitudes.

As seen from these figures, the number of half wave increases as the mode number increases.

4. Conclusions

The aim of this study is to analyze parametric earthquake analysis of reinforced concrete thick plates resting on Winkler foundation with using shear locking-free finite elements and to detect the effects of the thickness/span ratio, the aspect ratio and the boundary conditions on the linear responses of the reinforced concrete thick plates resting on Winkler foundation subjected to earthquake excitations. After the analysis it is detected that 17-noded finite element can be easy and effective used in the earthquake analysis of thick plates resting on elastic foundation without shear locking-problem and that if this element is used in an analysis, it is not necessary to use finer mesh. No matter what the mesh size is unless it is less than 4×4. The coded program can be effectively used in the earthquake analyses of any thick plates with Winkler foundation. In addition, it has generally been found that changing the thickness/span ratio in the plates is more effective than changing the aspect ratio in the maximum responses considered in this study.

For Winkler base coarse plates exposed to debris loading, both the frequency values of the earthquake load and the effects on the thickness/span ratio, aspect ratio and boundary conditions are somewhat difficult to interpret.

In order to generalize the values found in this study, the responses of the different thick plates with Winkler foundation subjected to different earthquake loading should be evaluated all together. Therefore, the curves presented herein can help the designer to estimate the effects of the thickness/span ratio, the aspect ratio, and the boundary conditions on the dynamic response of a thick plate with Winkler foundation.

The following conclusions can also be drawn from the results obtained in this study.

The changes in the aspect ratios are generally less effective on the absolute maximum displacement than the changes in the thickness/span ratios.

The changes in the aspect ratios are generally more effective on the absolute maximum bending moment, M_x, of the reinforced concrete thick simply supported plates than the changes in the thickness/span ratios.

The changes in the aspect ratios are generally more effective on the absolute maximum bending moment, M_x, of the reinforced concrete thick clamped plates resting on Winkler foundation than the changes in the thickness/span ratios.

The changes in the thickness/span ratios are generally more effective on the absolute maximum bending moment, M_y, of the reinforced concrete thick simply supported plates resting on Winkler foundation larger than the changes in the aspect ratios.

The changes in the thickness/span ratios are generally more effective on the absolute maximum bending moment, M_y, of the reinforced concrete thick clamped plates resting on Winkler foundation than the changes in the aspect ratios.

In general, degrees of decreases and increases depend on the changes in the aspect and thickness/span ratios, and thickness/span ratio was found to be more effective than the aspect ratio on the maximum responses considered in this study.

The frequency parameters increases with increasing b/a ratio for a constant value of *t/a* up to the 3rd frequency parameters, but after that the frequency parameters decreases with increasing *b/a* ratio for a constant value of *t/a*.

References

Ayvaz, Y., Daloğlu, A. and Doğangün, A. (1998), "Application of a modified Vlasov model to earthquake analysis of the plates resting on elastic foundations", *J. Sound Vib.*, **212**(3), 499-509.

Bathe, K.J. (1996), *Finite Element Procedures*, Prentice Hall, Upper Saddle River, New Jersey.
Cook, R.D., Malkus, D.S. and Michael, E.P. (1989), *Concepts and Applications of Finite Element Analysis*, John Wiley & Sons, Inc., Canada.
Grice, R.M. and Pinnington, R.J. (2002), "Analysis of the flexural vibration of a thin-plate box using a combination of finite element analysis and analytical impedances", *J. Sound Vib.*, **249**(3), 499-527.
Hetenyi, M. (1950), "A general solution for the bending of beams on an elastic foundation of arbitrary continuity", *J.Appl. Phys.*. **21**, 55-58.
Karasin, A. (2016), "Vibration of rectangular plates on elastic foundations by finite grid solution", *Int. J. Math. Comput. Meth.*, **1**, 140-145.
Kutlu, A., Uğurlu, B. and Omurtag, M.H. (2012), "Dynamic response of Mindlin plates resting on arbitrarily orthotropic pasternak foundation and partially in contact with fluid", *Ocean Eng*., **42**, 112-125.
Lok, T.S. and Cheng, Q.H. (2001), "Free and forced vibration of simply supported, orthotropic sandwich panel", *Comput. Struct*., **79**(3), 301-312.
Mindlin, R.D. (1951), "Influence of rotatory inertia and shear on flexural motions of isotropic, elastic plates", *J. Appl. Mech.*, **18**, 31-38.
Omurtag, M.H., Ozutok, A. and Akoz, A.Y. (1997), "Free vibration analysis of Kirchhoff plates resting on elastic foundation by mixed finite element formulation based on gateaux differential", *Int. J. Numer. Meth. Eng*., **40**, 295-317.
Ö zdemir, Y.I. (2012), "Development of a Higher Order Finite Element on a Winkler Foundation", *Finite Elem. Anal. Des.*, **48**, 1400-1408.
Ö zdemir, Y.I., Bekiroğlu, S. and Ayvaz, Y. (2007), "Shear locking-free analysis of thick plates using Mindlin's theory", *Struct. Eng. Mech.*, **27**(3), 311-331.
Pasternak, PL. (1954), "New method of calculation for flexible substructures on two-parameter elastic foundation", *Gasudarstvennoe Izdatelstoo. Literatury po Stroitelstvu I Architekture*, Moskau.
Senjanovic, I., Tomic, M., Hadzic, N. and Vladimir, N. (2017), "Dynamic finite element formulations for moderately thick plate vibrations based on the modified Mindlin theory", *Eng. Struct*., **136**, 100-113.
Sheikholeslami, S.A. and Saidi, A.R. (2013), "Vibration analysis of functionally graded rectangular plates resting on elastic foundation using higher-order shear and normal deformable plate theory", *Comput. Struct.*, **106**, 350-361.
Si, W.J., Lam, K.Y. and Gang, S.W. (2005), "Vibration analysis of rectangular plates with one or more guided edges via bicubic B-spline method", *Shock Vib*., **12**(5), 363-376.
Tahouneh, V. (2014), "Free vibration analysis of thick CGFR annular sector plates resting on elastic foundations", *Struct. Eng. Mech.*, **50**(6), 773-796.
Tedesco, J.W., McDougal, W.G. and Ross, C.A. (1999), *Structural Dynamics*, Addison Wesley Longman Inc., California.
Vlasov, V.Z. and Leont'ev, N.N. (1989), *Beam, Plates and Shells on Elastic Foundations*, GIFML, Moskau.
Weaver, W. and Johnston, P.R. (1984), *Finite Elements for Structural Analysis*, Prentice Hall, Inc., Englewood Cliffs, New Jersey.
Winkler, E. (1868), "Die Lehre von der Elastizität und Festigkeit mit besonderer Rücksicht auf ihre Anwendung in der Technik: für polytechnische Schulen, Bauakademien, Ingenieure, Maschinenbauer, Architecten, etc", Dominicius.
Wirowski, A., Michalak, B. and Gajdzicki, M. (2015), "Dynamic modelling of annular plates of functionally graded structure resting on elastic heterogeneous foundation with two modules", *J. Mech*., **31**(5), 493-504
Wu, L.H. (2012), "Free vibration of arbitrary quadrilateral thick plates with internal colums and uniform elastic edge supports by Pb-2 Ritz method", *Struct. Eng. Mech*., **44**(3), 267-288.
Wu, L.Y. and Lee, W.H. (2011), "Dynamic analysis of circular plates on elastic foundation by EFHT method", *J. Mech*., **19**(3), 337-347.
Zamani, H.A., Aghdam, M.M. and Sadighi, M. (2017), "Free vibration analysis of thick viscoelastic composite plates on Visco-Pasternak foundation using Higher-Order theory", *Comput. Struct*., **182**, 25-35.
Zenkour, A.M. and Radwan, A.F. (2016), "Free vibration analysis of multilayered composite and soft core sandwich plates resting on Winkler–Pasternak foundations", *J. Sandw. Struct. Mater.*, **20**(2), 1-22.
Zhang, C., Wang, B. and Zhu, Y. (2017), "Dynamic analysis of the infinite plate on orthotropic foundation subjected to moving loads", *J. Mater. Appl*., **6**(2), 63-69.
Zienkiewich, O.C., Taylor, R.L. and Too, J.M. (1971), "Reduced integration technique in general analysis of plates and shells", *Int. J. Numer. Meth. Eng*., **3**, 275-290.

AT